Chemistry & Biology
Article

Chemical Development of Intracellular Protein Heterodimerizers

Dominik Erhart,[1] Mirjam Zimmermann,[1] Olivier Jacques,[1] Matthias B. Wittwer,[2] Beat Ernst,[2] Edwin Constable,[3] Marketa Zvelebil,[4] Florent Beaufils,[1,*] and Matthias P. Wymann[1,*]
[1]Department of Biomedicine
[2]Department of Pharmaceutical Sciences
[3]Department of Chemistry
University of Basel, 4003 Basel, Switzerland
[4]The Institute of Cancer Research, London SW7 3RP, UK
*Correspondence: florent.beaufils@unibas.ch (F.B.), matthias.wymann@unibas.ch (M.P.W.)
http://dx.doi.org/10.1016/j.chembiol.2013.03.010

SUMMARY

Cell activation initiated by receptor ligands or oncogenes triggers complex and convoluted intracellular signaling. Techniques initiating signals at defined starting points and cellular locations are attractive to elucidate the output of selected pathways. Here, we present the development and validation of a protein heterodimerization system based on small molecules cross-linking fusion proteins derived from HaloTags and SNAP-tags. Chemical dimerizers of HaloTag and SNAP-tag (HaXS) show excellent selectivity and have been optimized for intracellular reactivity. HaXS force protein-protein interactions and can translocate proteins to various cellular compartments. Due to the covalent nature of the HaloTag-HaXS-SNAP-tag complex, intracellular dimerization can be easily monitored. First applications include protein targeting to cytoskeleton, to the plasma membrane, to lysosomes, the initiation of the PI3K/mTOR pathway, and multiplexed protein complex formation in combination with the rapamycin dimerization system.

INTRODUCTION

Chemical inducers of dimerization (CIDs) are powerful tools to specifically control protein homo- and heterodimerization (Corson et al., 2008). The most popular CID system currently uses rapamycin to dimerize FKBP12 and the FRB domain of mammalian target of rapamycin (mTOR), which results in the formation of a stable trimeric complex (Crabtree and Schreiber, 1996). Although the system displays excellent kinetics (Banaszynski et al., 2005), cross-reactions with the nutrient sensor mTOR complex 1 (TORC1) can occur. C16-derivatized rapalogs have been designed to interact only with mutated FRB domains, but not with endogenous mTOR (Liberles et al., 1997; Inoue et al., 2005; Edwards and Wandless, 2007). Using rapamycin and rapamycin derivatives (dubbed rapalogs), membrane translocation of lipid phosphatases was achieved targeting the plasma membrane (Varnai et al., 2006) and endosomes (Fili et al., 2006), while Inoue and Meyer successfully triggered PI3K activation by translocation (Inoue and Meyer, 2008). Minor contamination with rapamycin or rapamycin byproducts (<< 1%) can dramatically affect the PI3K/mTOR axis, which renders the rapamycin system less suitable for studies of growth control, immunity, and metabolism (Wullschleger et al., 2006).

The natural product coumermycin is a homodimerizer linking two amino-terminal subdomains of the B subunit of bacterial DNA gyrase (GyrB) on each side of the molecule (Mohi et al., 1998; O'Farrell et al., 1998). Several cellular signaling pathways were successfully targeted with the coumermycin system (Farrar et al., 1996; Mohi et al., 1998; Liu et al., 2000), but biological applications remain limited to homodimerization processes. CID based on dexamethasone (DEX) conjugated to methotrexate (MTX) or trimethoprim (TMP) have been introduced by the Cornish lab and were successfully used in a yeast three-hybrid system (Lin et al., 2000; Baker et al., 2002; Bronson et al., 2008). Phytohormone abscisic acid (ABA) stress response pathway proteins have recently been modified to control the proximity of cellular proteins (Liang et al., 2011). The ABA-induced CID system offers the advantage that it relies on binding partners that have no endogenous counterparts, but so far no rapid dimerization has been demonstrated. Furthermore, most of the systems discussed in Corson et al., 2008, including the ABA system, depend on reversible noncovalent interactions, which render the quantification of successful dimerization challenging.

The use of self-labeling technologies allows the covalent incorporation of a wide range of modifications at specific protein sites (Hinner and Johnsson, 2010). Mutants of the DNA repair protein O6-alkylguanine-DNA-alkyltransferase (SNAP-tag and CLIP-tag) transfer alkyl groups from their substrates, such as O6-benzylguanine (BG; Keppler et al., 2003) and O6-benzylcytosine (BC; Gautier et al., 2008), to a reactive Cys residue. Haloalkane dehalogenase (HaloTag) has been designed to covalently bind to synthetic chloroalkane ligands (Los et al., 2008). Covalent bond formation between these protein tags and their targeted compounds is highly specific, occurs rapidly under physiological conditions, and is essentially irreversible. Johnsson and coworkers have developed hetero-bisfunctional BG-MTX heterodimerizers, which were successfully used to control transcription

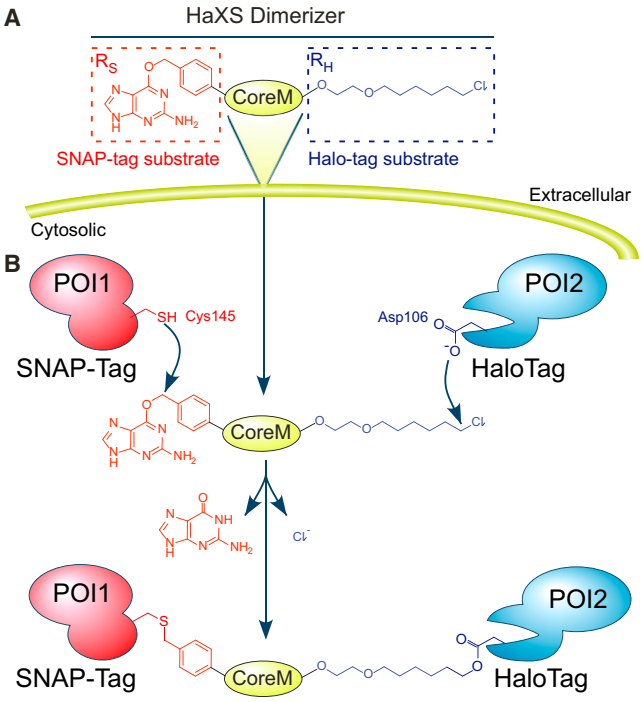

Figure 1. Schematic Representation of Chemically Induced Dimerization of Intracellular Proteins by HaXS Molecules

(A) HaloTag and SNAP-tag substrate moieties were integrated into bivalent reactive cross-linking molecules (HaXS). The O6-benzylguanine function (red, R_S in subsequent figures) reacts with Cys145 in the SNAP-tag, while the chloroalkane (blue, R_H) links to Asp106 in the HaloTag.

(B) HaXS dimerizer molecules were rendered cell permeable by the integration of specifically designed features into the core module (CoreM) of HaXS dimerizers. Once HaXS enter cells, they heterodimerize exogenously expressed proteins of interest (POIs) fused to SNAP- and HaloTags. In contrary to other covalent chemical dimerizers, HaXS molecules link tagged proteins even if they are not pre-associated (see Figure S1 and Table S1).

in yeast (Gendreizig et al., 2003). The same group produced a SNAP-homodimerizer (CoDis; Lemercier et al., 2007) and bivalent fluorescent substrate S-CROSS, linking SNAP- and CLIP-tagged proteins (Gautier et al., 2009). Like for the covalent homodimerizer xCrAsH, which targets tetracysteine tags (Rutkowska et al., 2011), S-CROSS links exclusively pre-associated binding partners. Although xCrAsH is suited for intracellular applications, S-CROSS reactivity has only been demonstrated in cell lysates so far.

An alternative approach to control protein-protein interactions locally is provided by genetically encoded light-inducible protein dimerizing systems (Yazawa et al., 2009; Kennedy et al., 2010; Idevall-Hagren et al., 2012; Strickland et al., 2012). They offer an unprecedented speed of dimerization (Idevall-Hagren et al., 2012). Large protein tags (e.g., FKF1 with 1173 amino acids [Yazawa et al., 2009] or PhyB with 908 amino acids [Levskaya et al., 2009]), and sensitivity to accidental exposure to green/blue light, favor the application of these systems in imaging, but obstruct biochemical investigation of triggered interactions.

Here, we show the development and applications of an alternative dimerization strategy based on a class of covalent chemical cross-linkers fusing HaloTag and SNAP-tag substrates (HaXS; Figure 1A; Figure S1 and Table S1 available online). This tag combination profits from a high reaction rate of the HaloTags and SNAP-tags with their respective substrates (Hinner and Johnsson, 2010) and attains high selectivity inside mammalian cells. The strategy unites efficient covalent protein dimerization with optimized cell permeability in HaXS molecules and provides a simple control and workup of CID-induced complexes (Figure 1B).

RESULTS AND DISCUSSION

Intracellular cross-linkers need to combine tag reactivity and cell permeability. Because tag reactivity has been optimized before, the core module linking SNAP-tag and HaloTag substrates was left as a point of attack to modify physicochemical properties of HaXS molecules. A progressive chemical optimization of the core module included the integration of groups modulating water solubility and cell permeability, and of bulky or semirigid structures separating the two tag-reactive moieties (for schematics, see Figure 1B).

Structural Analysis of Core Module Properties and Improvement of Cell Permeability of HaXS Molecules

To explore the required length of alkyl and PEG elements between HaloTag and SNAP-tag substrates, compounds HaXS1 and HaXS2 (Figure 2A) were tested in cellular systems. In HeLa cells transiently transfected with SNAP-GFP and Halo-GFP fusion proteins, optimal HaXS1 or HaXS2 concentrations (5 μM) yielded up to 40%–50% intracellular dimerization. The elongation of the core module in HaXS2, as compared to HaXS1, improved cross-linking at elevated concentrations and incubation times (Figures 2B and 2C). The observation that time-resolved dimerization curves of HaXS1 and HaXS2 match initially ($t < 1$ hr, Figure 2C) and the fact that HaXS1 has a higher cell permeability than HaXS2 as determined in a permeability assay (see below) suggest that the faster diffusion rate of HaXS1 could initially compensate its inferior reactivity (compared to HaXS2), while the longer HaXS2 yields higher dimerization efficiencies at later time points (at 4 hr > 50% for HaXS2, 25% for HaXS1). The better cell permeability and inferior dimerization capacity of HaXS1 also explains why high concentrations of HaXS1 (50 μM) counteracted the formation of heterodimeric HaloTag-SNAP-tag complexes, most likely by masking reactions generating increasing levels of monomeric, reacted Halo- and SNAP-GPF species (Figure 2B), which was not observed with high concentrations of HaXS2.

These results suggest that intracellular dimerization reaction is best interpreted as a convolution of substrate/tag reactivity and limited diffusion of the compounds into intracellular space. This view is also supported by the extended time required to reach relevant yields of intracellular dimerization with this first-generation HaXS molecules, as compared to previously reported single sided reaction rates of HaloTag and SNAP-Tag with their specific substrates (3×10^6 $M^{-1} \cdot s^{-1}$ and 3×10^4 $M^{-1} \cdot s^{-1}$, respectively; Hinner and Johnsson, 2010). These pilot studies with HaXS1 and HaXS2 made it clear that a minimal core module size is crucial to efficiently cross-link the Halo-GFP and SNAP-GFP fusion proteins, and that cell permeability needs to be improved for faster intracellular reactivity.

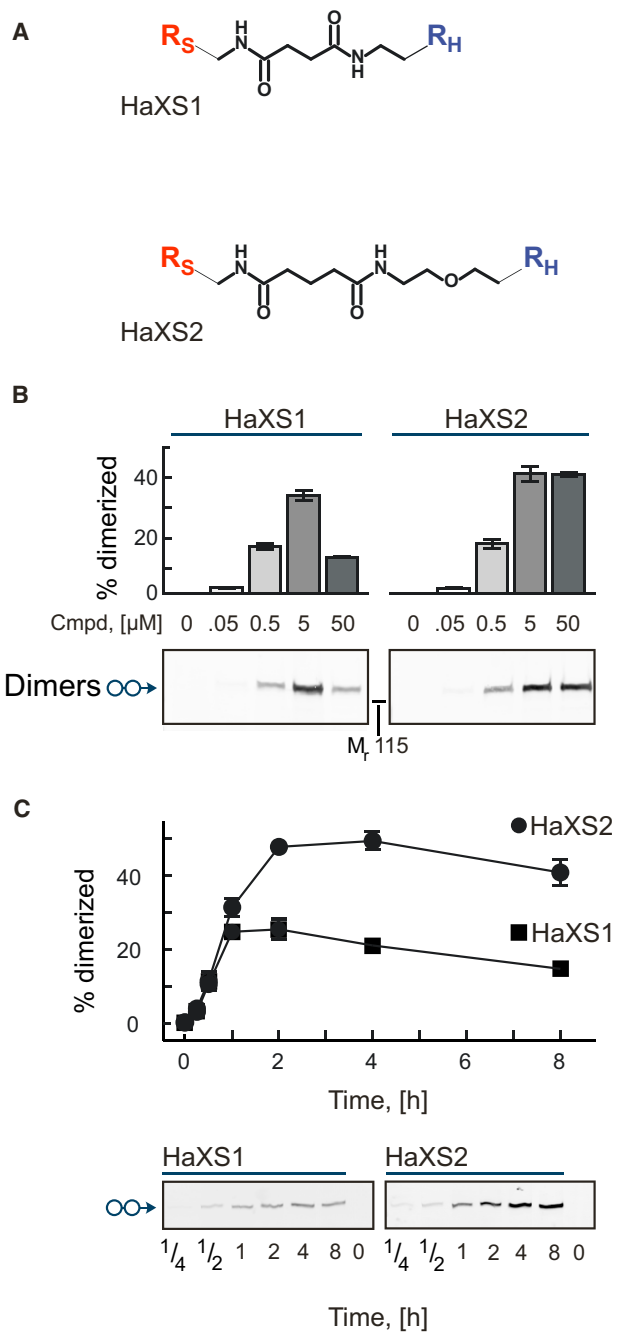

Figure 2. Intracellular Heterodimerization Induced by First-Generation HaXS Molecules

(A) Abbreviated structure (for R_S and R_H see Figure 1) of the bisfunctional HaloTag and SNAP-tag reactive molecules HaXS1 and HaXS2.

(B) HeLa cells transfected with expression constructs for SNAP-GFP and Halo-GFP (see Supplemental Experimental Procedures) were exposed to HaXS1 and HaXS2 at the indicated concentrations for 1 hr at 37°C in complete cell culture medium, before cells were lysed and proteins were subjected to SDS-PAGE and immune-blotting for SNAP/HaloTag dimers using anti-GFP (primary) and fluorescently-labeled (secondary) antibodies to generate a readout on an infrared imaging system.

(C) HeLa cells (cotransfected with SNAP-GFP and Halo-GFP as in (B) were incubated with the indicated HaXS compound (5 μM), and lysed at the indicated time for analysis of dimers as in (B). Quantifications of the concentration and time-dependent heterodimerization are means ± SEM of three independent experiments. Error bars were removed where smaller than the symbols used. A detailed description of the synthesis of HaXS molecules can be found in the Supplemental Experimental Procedures.

Second-generation HaXS molecules were designed on the basis of a HaXS2 scaffold aimed to maintain comparable core module size and low molecular weight, while introducing features to improve cell permeability. Along these lines, HaXS3 was designed to replace the central glycine moiety with functionalized amino acids, and to generate a HaXS library (Figure 3A). Because fluorinated groups have been reported to modulate physicochemical properties of molecules considerably (Böhm et al., 2004), we produced alkylated and fluorinated analogs of HaXS3 to integrate a lipophilic surface as an entry point into cellular membranes. To further investigate the influence of fluorine substitutions on cell penetration of HaXS3 derivatives, fluorinated and nonfluorinated analogs were produced in parallel: alkyl-analog HaXS4 and fluorinated HaXS5 were synthesized by the exchange of the glycine moiety included in the HaXS3 core structure by methylalanine or trifluoromethylalanine groups, respectively. The phenyl-analogs HaXS6 and the corresponding fluorinated HaXS7 were made according to the same strategy from Fmoc-phenylalanine or Fmoc-pentafluorophenylalanine (Figure 3A). HaXS3 has comparable intracellular dimerization efficiency compared to first-generation HaXS molecules. The simple alkyl chain introduced in HaXS4 led to a reduction of intracellular dimerization as compared to HaXS3 and HaXS2, but the trifluoromethylated HaXS5 rescued dimerization of Halo-GFP and SNAP-GFP fusion protein back to 40% within 1 hr. The lipophilic nature of the phenyl group in HaXS6 and the pentafluorophenyl group in HaXS7 improved cell penetration even further. The nonfluorinated aryl derivative HaXS6 showed characteristics matching those of the fluorinated HaXS5 molecule. Significant progress in rate and efficiency in intracellular dimerization was achieved with the pentafluorophenyl derivative HaXS7 (Figures 3B and 3C).

Based on results from the above HaXS series, a third-generation dimerizer was envisaged: assuming that HaXS molecules are delivered inside cells via passive diffusion through cell membranes, we next targeted a dimerizer with a lower molecular weight, and thus synthesized a flat derivative of HaXS7. One of the emerging strategies was to integrate the polyfluorophenyl substituent from HaXS7 into the core module structure. HaXS8 was synthesized in six steps from tetrafluorohydroquinone, tetraethylene glycol, BG-NH2, and 6-chloro-1-iodohexane (Figure 4A) with a good overall yield (1 g produced in total; see Supplemental Experimental Procedures available online). Additionally, minimization of core module flexibility aimed to prevent steric clashes during the formation of the protein complex, hereby allowing higher yields of Halo-GFP and SNAP-GFP dimerization. Molecular modeling was performed to eliminate the possibility that the designed molecules would link the HaloTag and the SNAP-tag in a way to generate unfavorable steric clashes between the two tags. As shown in Figure 4B, HaXS8 provided a fair amount of degrees of freedom to arrange the HaloTag and the SNAP-tag proteins in the docked complex, suggesting that HaXS8 provided sufficient core module size and flexibility for optimal docking.

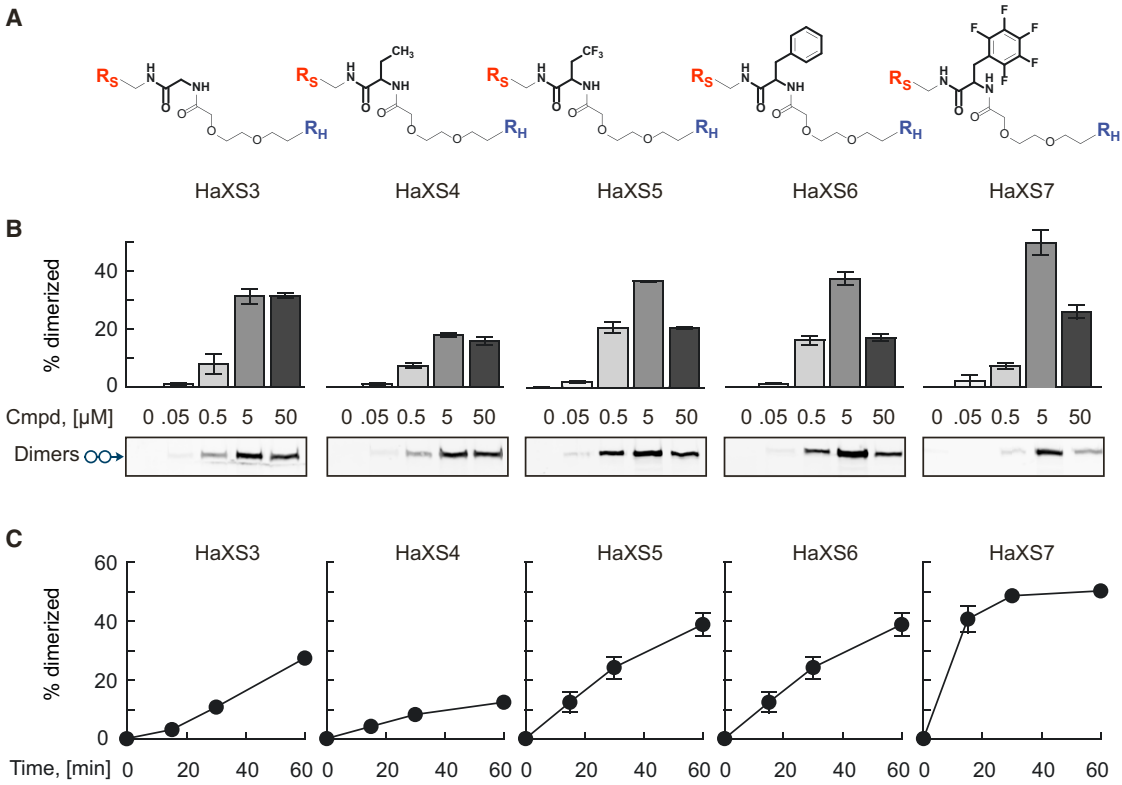

Figure 3. Intracellular Dimerization Triggered by Second-Generation HaXS Molecules—Influence of Concentration and Time of Exposure

(A) Abbreviated structures of fluorinated and nonfluorinated bisfunctional Halo- and SNAP-tag reactive molecules.

(B) HeLa cells co-expressing SNAP-GFP and Halo-GFP were exposed to the indicated amounts of HaXS compounds for 1 hr at 37°C (for details see Figure 2C and Supplemental Experimental Procedures).

(C) HeLa cells expressing SNAP-GFP and Halo-GFP fusion proteins were incubated with 5 μM of the indicated HaXS molecules, before they were lysed at the given times for detection of dimerization by immune-blotting (as in Figure 2C). Values represent the mean of three independent experiments ± SEM.

In HeLa cells, intracellular dimerization of Halo-GFP and SNAP-GFP fusion proteins reached > 65% with HaXS8, notably already at 10-fold lower concentrations of the compound as compared to HaXS2 and HaXS7 (Figure 4C). Differences between HaXS8 and earlier generation HaXS molecules became even more prominent at lower concentrations, as HaXS8 displayed significant intracellular dimerization as low as 50 nM, where none of the other HaXS molecules displayed significant dimerization. Moreover, HaXS8 was capable of dimerizing > 50% of tagged proteins over a wide concentration range. This exceeds values typically achieved for surface receptor/signaling chain interactions by a factor of around 10×, as receptors recruit cytosolic components in the low percentage range (Deswal et al., 2011).

To correlate cell permeability and the performance in intracellular dimerization reactions directly, we performed a parallel artificial membrane permeability assay (PAMPA; for a review see Faller, 2008) with all HaXS molecules (Figure 4E). A correlation between the obtained permeability values (P_e) and the intracellular dimerization obtained for each HaXS compound showed that cell permeability is indeed a key factor for an efficient heterodimerization process in cells. HaXS1 is the only outlier in this analysis, as the compound has the lowest molecular weight contributing to improved membrane permeability, but reduced coupling reactivity due to steric constraints.

Protein Translocation to Selected Cellular Compartments

Using HaXS8, we next aimed to target tagged proteins to specific locations inside living cells. As a first approach, tagged fusion proteins of actin (SNAP-Actin) and GFP (Halo-GFP) were co-expressed in NIH 3T3 cells. These cells form stress fibers, which contain filamentous actin (F-actin), and can be visualized with the F-actin stain rhodamine-phalloidin. Upon addition of HaXS8, Halo-GFP was translocated to stress fibers, and colocalized with rhodamine-phalloidin staining, which was confirmed by image analysis of cross-linked Halo-GFP/SNAP-Actin complexes (Figure 5A).

In parallel, HaXS8 controlled the translocation of fluorescent fusion proteins from the cytoplasm to the plasma membrane in MDCK epithelial cells: cytosolic red fluorescent protein (monomeric RFP; TagRFP) was expressed as HaloTag fusion protein (Halo-RFP), and a membrane anchor was constructed fusing a SNAP-tag, GFP, and the isoprenylation sequence from KRas4B (the CAAX box), which targeted the resulting SNAP-GFP-CAAX fusion protein exclusively to the plasma membrane. When MDCK cells, expressing SNAP-GFP-CAAX and Halo-RFP,

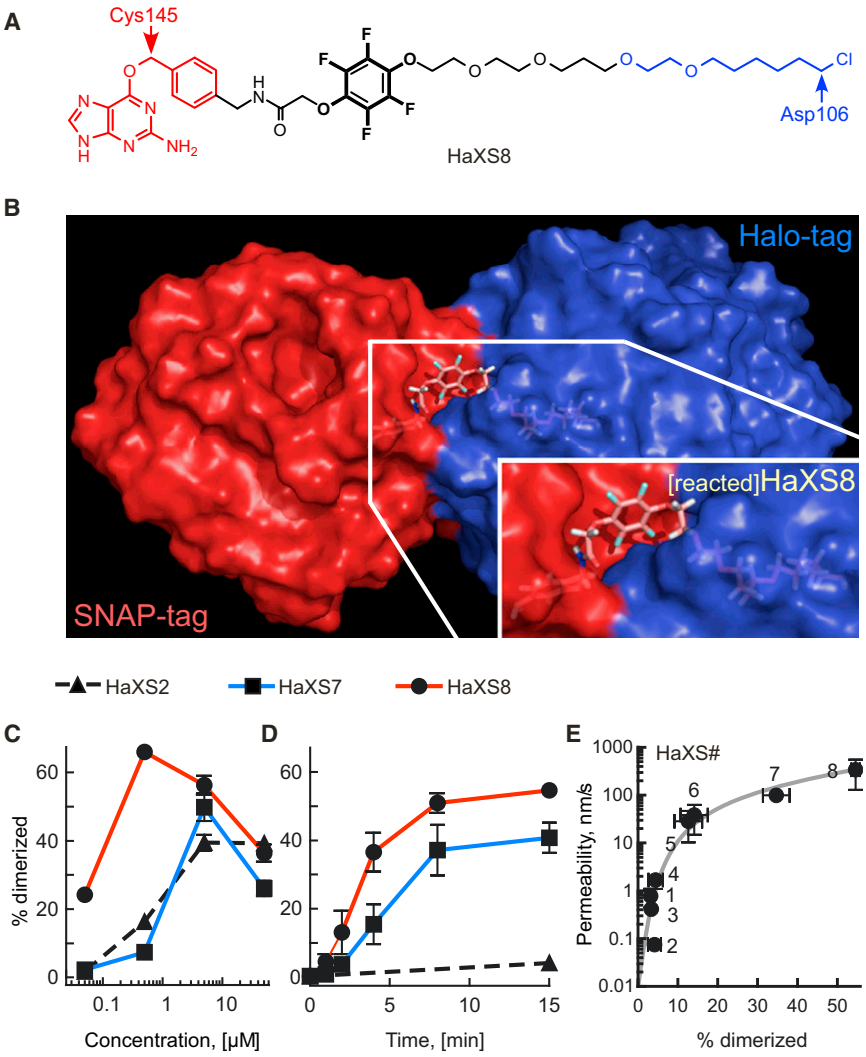

Figure 4. The Structurally Optimized Dimerizer HaXS8 in Comparison with the First- and Second-Generation HaXS Compounds

(A) Chemical structure of the optimized bisfunctional HaloTag and SNAP-tag reactive molecule HaXS8.

(B) Modeled structure of a covalently linked HaloTag-[reacted]HaXS8-SNAP-tag adduct. The [reacted]HaXS8 molecule (elimination of guanine and Cl^-, see Figure 1) was linked to Cys145 in the SNAP-tag (red) and to Asp106 in the HaloTag (blue) crystal structures, before randomized structural starting points were put through energy minimization (see Supplemental Experimental Procedures). Depicted is a sample structure representing a tight fit between HaloTag and SNAP-tag, which leaves the alkane chain within the HaloTag entry tunnel in a relaxed conformation.

(C) HeLa cells co-expressing SNAP-GFP and Halo-GFP were incubated in complete medium with HaXS8, HaXS7, or HaXS2 at the indicated concentrations for 1 hr at 37°C before cell lysis (see Figure 2C).

(D) HeLa cells as in (C) were exposed to 5 μM of HaXS8, HaXS7, or HaXS2 for the indicated time, before cells were lysed and probed for HaloTag and SNAP-tag dimerization (all values are means of three individual experiments ± SEM).

(E) All HaXS compounds presented here were subjected to an artificial membrane permeability assay (PAMPA; see Supplemental Experimental Procedures) to assess cell permeability (expressed as P_e, [nm/s]). P_e was plotted logarithmically against the percentage of intracellular dimerization achieved after a 15 min exposure of HeLa cells (as in C) to the indicated HaXS compounds at 5 μM (labeled 1–8; n = 3; mean ± SEM).

were incubated with HaXS8, the initially cytosolic Halo-RFP protein was relocated to the plasma membrane (Figure 5B).

Chemical Induction of Intracellular Signaling

Protein/membrane interactions play a major role in the activation of cellular signaling cascades in physiology and disease (Wymann and Schneiter, 2008). Overactivation of phosphoinositide 3-kinase (PI3K) has gained much attention because it contributes to the promotion of cancer and inflammation (Cantley, 2002; Wymann and Marone, 2005; Zoncu et al., 2011; Wymann, 2012). Class IA PI3Ks are composed of a regulatory p85 and a catalytic p110 kD subunit. The p85 subunit docks with two src-homology 2 (SH2) domains to phosphorylated tyrosines on activated growth factor receptors and drags the catalytic p110 subunit via a coiled-coil domain located between the two SH2 domains (dubbed inter-SH2, or iSH2; for structural schemes see Wymann et al., 2003) to the membrane. PI3K then produces phosphatidylinositol(3,4,5)-trisphosphate [PtdIns(3,4,5)P_3], a lipid that serves as a plasma membrane docking site for signaling enzymes containing pleckstrin homology (PH) domains. Phosphoinositide-dependent kinase-1 (PDK1) and protein kinase B (PKB/Akt) both contain PtdIns(3,4,5)P_3-binding PH domains. PDK1 directly phosphorylates PKB/Akt on Thr308, while a secondary site on PKB/Akt (Ser473) is phosphorylated by mTOR complex 2 (TORC2). When fully activated, PKB/Akt takes a major role in the activation of TORC1, and active TORC1 phosphorylates p70 S6 kinase ($p70^{S6K}$) on Thr389.

Rapamycin derivatives have been reported to boost a feedback leading to the amplification of PI3K signaling upstream of TORC1 (O'Reilly et al., 2006), which provides a reason to validate the HaXS strategy in the PI3K/mTOR pathway: a SNAP-GFP-CAAX anchor in the plasma membrane (see above) served as the docking site for a HaloTag protein fused to the inter-SH2 domain of p85 (Halo-iSH2-GFP; Figure 6A). The addition of HaXS8 to HEK293 cells induced a rapid and efficient cross-linking of the membrane anchor and the iSH2 construct, and triggered the activation of the downstream targets PKB/Akt (as monitored by Thr308 and Ser473 phosphorylation on PKB/Akt) and mTOR (monitored by phosphorylation of T389 of p70 S6 kinase, $p70^{S6K}$ by TORC1). Although typical growth factor stimulation also induces an activation of the MAPK pathway, HaXS8

did not upregulate MAPK phosphorylation, demonstrating that the system can be used to selectively induce isolated signal transduction branches (Figure 6B).

Control experiments forcing the dimerization of a cytosolic SNAP-GFP with the Halo-iSH2-GFP did not activate the PI3K/mTOR pathway, illustrating that membrane proximity of the iSH2/p110 PI3K complex was crucial to relay downstream signals. Moreover, HaXS8 did not interfere with mTOR signaling induced by serum stimulation. Rapalog-based CID systems can generate a distorted output in this system (see Figure S2 and Supplemental Experimental Procedures). Although HaXS8 does not yet match the dimerization rates attained with rapalog CID systems, it offers the advantage that numerous connections within the PI3K/mTOR pathway can be explored without interference during long term stimulation.

Multiplexing Applications

It can also be envisaged that the HaXS dimerizers can be applied orthogonally in conjunction with other CID systems, as this has been elegantly demonstrated for the combination of rapamycin and gibberellin analogs recently (Miyamoto et al., 2012). Such combinations allow the construction and alignment of sophisticated enzymatic reaction chains that can be utilized to probe complex signaling pathways. A proof-of-concept approach combining a pre-dimerization step mediated by HaXS8, followed by a rapamycin-induced translocation of the preformed Halo/SNAP-tag complex to a lysosomal anchor protein containing LAMP1 (LAMP-CFP-FRB), is shown in Figure 7. Successful translocation of a cytosolic Halo-RFP fusion protein to lysosomes was only observed in the presence of HaXS8 and rapamycin, as a FKBP-SNAP protein acted as a bridge from Halo-RFP to the membrane anchor (see Figure 7B for a scheme of the docked complexes). Although only two fluorescent proteins (CFP and RFP) were used as cargo to monitor selective translocation, up to three cargo proteins or enzymes can be easily integrated into the setup.

As for other CID systems, tag fusions and probe constructs need to be considered carefully when using HaXS8 molecules to dimerize HaloTag and SNAP-tag fusion proteins. While noncovalent CID assemblies can only be rated and modified by their expected cellular output, covalent complexes can be easily detected in the HaXS system, and success of dimerization can be validated, and correlated with signal output and subcellular targeting directly. In contrast to other covalent systems (see S-CROSS and xCrAsH), HaXS8 can force dimerization of previously noninteracting proteins, and has been specifically optimized for cellular permeability.

SIGNIFICANCE

The cell-permeable HaXS molecules promote a covalent intracellular dimerization of HaloTag and SNAP-tagged proteins of interest. The covalent and irreversible nature of the reaction of the chemical dimerizer with HaloTag and SNAP-tag allows easy monitoring of the dimerization process even under denaturing conditions. The design and chemical development of HaXS compounds focused on the optimization of cellular availability and reactivity. Although previously described covalent protein dimerizers were used to confirm well-known protein-protein interactions, HaXS molecules have the ability to force protein-protein interactions. As shown here, forced protein complex formation can also be exploited to promote protein translocation to different cellular compartments, and to activate distinct cellular signaling pathways. In contrary to the widely used rapalog CID systems, HaXS compounds can be utilized to trigger PI3K/mTOR signaling pathways, without interference with endogenous signaling molecules and induction of feedback mechanisms. HaXS molecules can be used in combination with other (noncovalent) dimerization systems, and thus extend the possibilities to devise multiplexing approaches, and to chemically control the assembly of elaborate protein complexes and signalosomes.

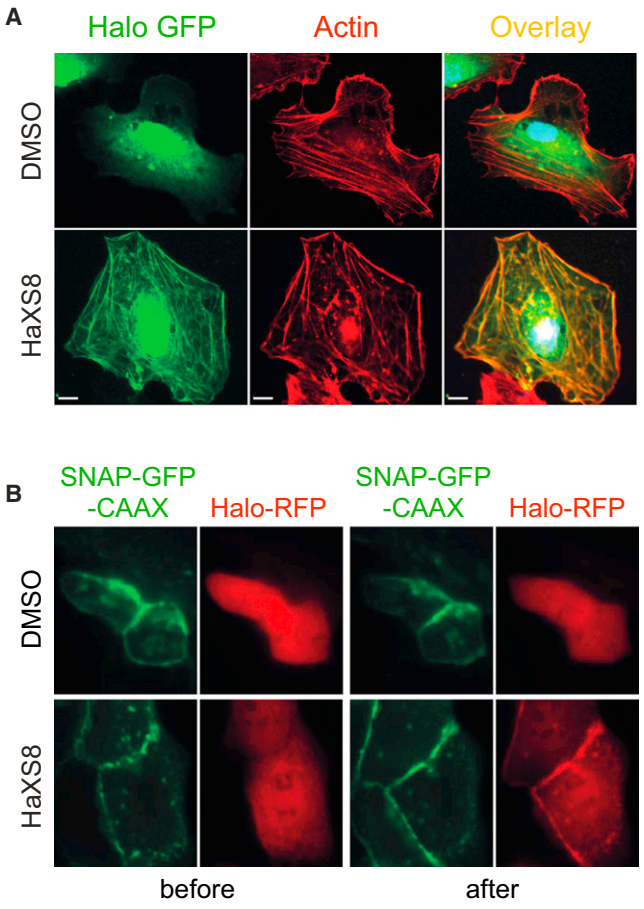

Figure 5. Protein Translocation to Specific Cellular Compartments

(A) NIH 3T3 cells expressing SNAP-Actin and Halo-GFP (green) fusion proteins were incubated with DMSO or 0.5 μM HaXS8 for 1 hr at 37°C. Rhodamine-phalloidin was used to visualize F-actin in stress fibers (Actin, red). Translocation of GFP to the actin cytoskeleton was imaged by confocal microscopy on live cells.

(B) MDCK cells expressing a SNAP-GFP-CAAX membrane anchor (green [-CAAX is the polybasic isoprenylation sequence from KRas-4B]) and Halo-RFP (red) fusion protein were incubated with DMSO or 0.5 μM HaXS8 in complete medium for 40 min at 37°C. Translocation of Halo-RFP to the plasma membrane was imaged by confocal microscopy on live cells.

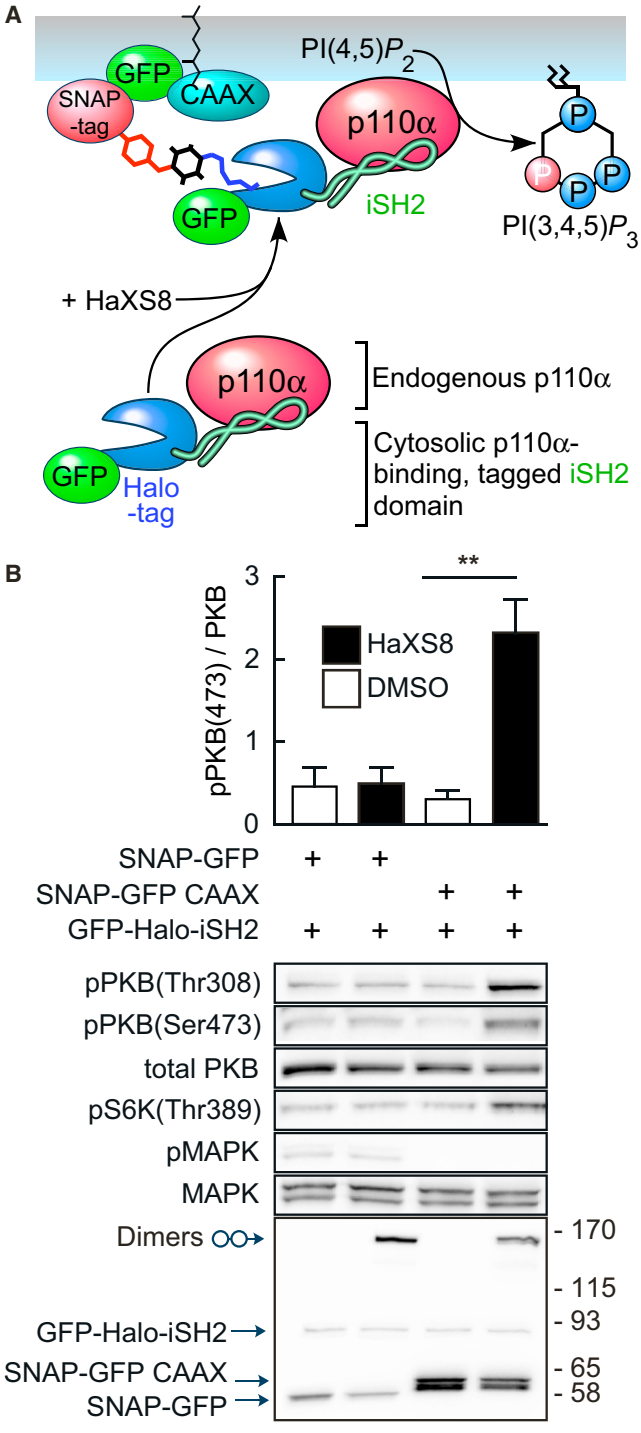

Figure 6. Activation of the PI3K/mTOR Pathway by Chemically Induced Membrane Targeting

(A) Schematic representation of the translocation process recruiting a cytosolic iSH2 domain (derived from the PI3K regulatory PI3K subunit p85, see text) fused to the HaloTag to a membrane anchored SNAP-tag using HaXS8. PI3Ks activity at the membrane forms PtdIns(3,4,5)P_3 [PI(3,4,5)P_3] from PI(4,5)P_2, followed by specific activation of PI3K/PKB/mTOR pathway.

(B) HEK293 cells were cotransfected with SNAP-GFP-CAAX (from KRas4B) and iSH2 fused to Halo-GFP. HEK293 cells expressing SNAP-GFP-CAAX and iSH2-Halo-GFP were starved overnight, and exposed to DMSO or 0.5 μM HaXS8 in complete medium for 40 min, before cell lysis and signaling pathway analysis using the indicated phosphor-specific antibodies. Control experiments included cytosolic SNAP-GFP constructs. SNAP/HaloTag dimers were detected as described previously. Quantifications of signal intensities represent the mean of ± SEM of two independent experiments. HaXS8 does not interfere with PI3K/mTOR signaling (see Figure S2).

EXPERIMENTAL PROCEDURES

Synthesis

Detailed synthetic procedures, materials and reagents, and characterizations for all compounds are described in the Supplemental Experimental Procedures.

Protein Denaturation, Cell Lysis, and Immunoblotting

Cells were washed with ice cold PBS and lysed in a NP-40 lysis buffer (1% NP-40, 20 mM Tris-HCl pH 8.0, 138 mM NaCl, 2.7 mM KCl, 5% glycerol, 40 mM NaF, 2 mM Na_3VO_4, 20 μM Leupeptin, 18 μM Pepstatin, 5 μM Aprotinin, 1 mM PMSF, 1 mM $MgCl_2$, 1 mM $CaCl_2$, 5 mM EDTA). Cell lysates were cleared by centrifugation at 13,000 rpm for 15 min and proteins were denatured by the addition of 5× sample buffer (312.5 mM Tris-HCl [pH 6.8], 10% SDS, 25% β-mercaptoethanol, 50% glycerol, bromphenol blue) and boiling for 6 min. Proteins were separated by SDS-PAGE, and transferred to Immobilon PVDF membranes (Millipore). Mouse monoclonal antibody (mAb) to pThr389-S6K, rabbit mAb to S6K1, mouse mAb to pSer473-PKB/Akt and to pThr308-PKB/Akt (all from Cell Signaling Technology, Danvers), mouse mAb to PKB (kind gift of E. Hirsch, Turin, Italy), mouse mAb to pMAPK and rabbit mAb to MAPK (both from Sigma-Aldrich), mouse mAb to HA (HA.11, Babco), and GFP (Roche Diagnostics) were used to detect proteins by immunoblotting. Secondary antibodies were either labeled with Alexa Fluor 680 (LI-COR) for detection on an Odyssey (LI-COR) infrared imaging system, or were horseradish peroxidase (HRP)-conjugated goat antimouse IgG and goat anti-rabbit IgG (Sigma) for visualization using enhanced chemiluminescence (Millipore) detected by a CCD camera system (Fusion Fx7, Vilber).

Cloning and Expression of Recombinant Proteins

The HaloTag7 coding sequence (Promega), SNAP-tag (pSS26m) coding sequence (Covalys), iSH2 domain coding sequence (Addgene), actin coding sequence (Clonetech), and EGFP coding sequence (Clonetech) were amplified by PCR (Phusion polymerase, Finnzymes) and transferred to pcDNA3 (Invitrogen), pTagRFP-N1 (Evrogen; expression vector for a monomeric TagRFP, here short RFP from sea anemone Entacmaea quadricolor [Merzlyak et al., 2007]), pEGFP (Clonetech) with excised GFP or pEGFP-C3 (Clonetech) vectors for expression. For recombinant protein production, Halo-EGFP and SNAP-EGFP were cloned into pTriEx-4 (Novagen) and expressed as N-terminal $(His)_6$ fusion proteins, and purified on Ni^{2+}-NTA beads (QIAGEN) according to the manufacturer's instructions.

To generate a Halo-FRB expression construct, CLIP was exchanged in a CLIP-FRB plasmid (Gautier et al., 2009) by the Halo sequence. The Halo-FRB and SNAP-FKBP (Gautier et al., 2009) cassettes were then transferred into a pcDNA3 (Invitrogen) backbone containing an N-terminal HA-tag in the multicloning site. The LAMP-CFP-FRB plasmid is described in (Komatsu et al., 2010).

Cell Culture and Transfection

HeLa, HEK293, MDCK, and NIH 3T3 (originally from ATCC) were cultured in complete Dulbeccos's modified Eagle medium (DMEM) with 10% heat-inactivated fetal calf serum (HIFCS), 2 mM L-glutamine (Gln), 1% penicillin-streptomycin solution (PEST) at 37°C, and 5% CO2. Transfections were carried out with JetPEI (Brunschwig) according to the manufacturer's guidelines.

Cellular Heterodimerization and Biological Induction

One day after transfection of HeLa cells with expression constructs for SNAP-GFP, SNAP-GFP-CAAX, Halo-RFP, Halo-GFP, LAMP-CFP-FRB, HA-SNAP-FKBP, or SNAP-Actin, cells were exposed to HaXS dimerizers at the indicated concentrations for indicated times at 37°C in fully supplemented complete

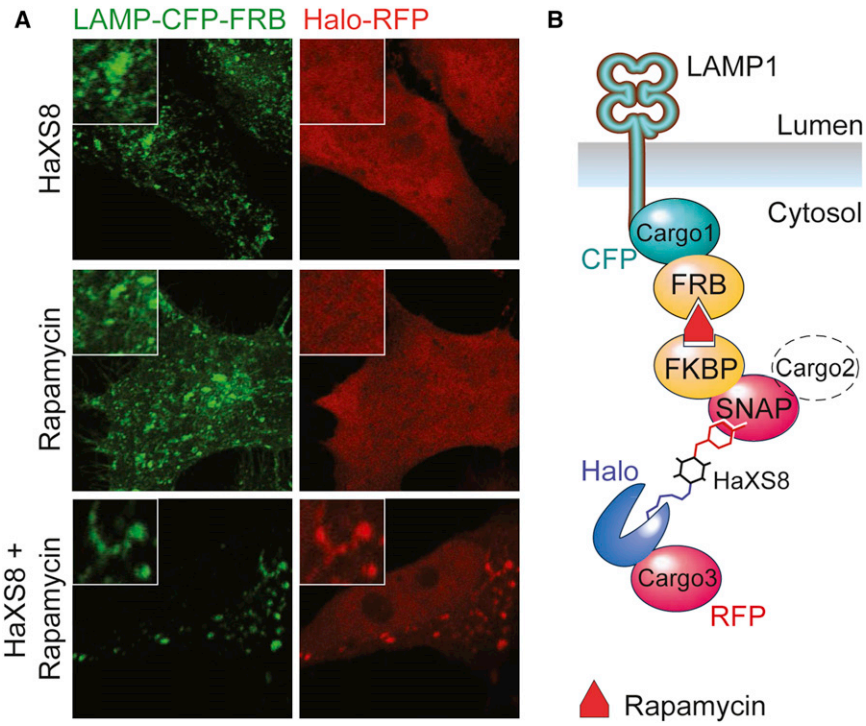

Figure 7. An Orthogonal Application of the HaXS System in Combination with Rapamycin-Mediated Protein Dimerization

(A) HeLa cells co-expressing LAMP-CFP-FRB (green), SNAP-FKBP, and Halo-RFP (red) were first exposed to 0.5 μM HaXS8 for 1 hr, followed by 0.5 μM rapamycin for 5 min, where indicated. Subsequently, cells were fixed and pictured by confocal microscopy.

(B) Schematic representation of the docked and assembled multimeric complex: cytosolic Halo-Tag fused to RFP (Cargo3) can form a covalent link to a SNAP-FKBP fusion protein via the reaction with HaXS8. This complex (which could be extended by Cargo2) is still cytosolic. Once rapamycin is added, the complex is targeted to a FRB-tagged anchor (here LAMP-CFP-FRB) at specific cellular locations (here lysosomal membranes) via the FKBP-rapamycin-FRB interaction.

DMEM medium. For immunoblot analysis, cells were lysed, and proteins were separated by SDS-PAGE. SNAP-tag/HaloTag dimers were detected using anti-GFP (primary) and fluorescently labeled (secondary) antibodies, and measured on the Odyssey infrared imaging system. For microscopy transfected cells were grown on 12 mm coverslips (Menzel), treated with DMSO or HaXS8, washed twice with PBS, fixed with 4% *p*-formaldehyde (PFA) in PBS, and mounted in Mowiol (Plüss-Stauffer) containing 1% propyl gallate (Sigma-Aldrich). For staining of F-actin, cells were permeabilized in PBS, 1% BSA, 0.1% Triton X-100, and incubated with rhodamine-phalloidin (Molecular Probes).

For the studies of PI3K/mTOR signaling, HEK293 cells were cotransfected with SNAP-GFP-CAAX and iSH2 fused to Halo-GFP. One day after transfection, cells were serum-starved overnight. After a 40 min exposure with 0.5 μM HaXS8 cells were lysed for the analysis of signal pathway induction, and the formation of HaloTag/SNAP-tag dimers.

For live cell microscopy, transfected cells grown on coverslips were mounted in life-microscopy chambers (Life Imaging Services) in a closed confirmation with complete medium. Images were acquired on an Axiovert 200 M microscope (Zeiss) fitted with a Plan-Achromat 63×/1.4 oil objective and an Orca ER II camera (Hamamatsu), and operated by OpenLab software (Perkin Elmer).

SUPPLEMENTAL INFORMATION

Supplemental Information includes Supplemental Experimental Procedures, two figures, and one table and can be found with this article online at http://dx.doi.org/10.1016/j.chembiol.2013.03.010.

ACKNOWLEDGMENTS

We thank T. Wandless for iRap, and B. Giese for valuable advice and discussions, T. Inoue for the LAMP-CFP-FRB expression plasmid, and K. Johnsson for FRB- and FKPK domain-containing plasmids. This work was supported by Swiss National Science Foundation grants 205320-138302 and 31EM30-126143, the ESF EuroMEMBRANE programme grant FP-018, and the Novartis (Jubilée) Foundation.

Received: January 8, 2013
Revised: March 13, 2013
Accepted: March 20, 2013
Published: April 18, 2013

REFERENCES

Baker, K., Bleczinski, C., Lin, H., Salazar-Jimenez, G., Sengupta, D., Krane, S., and Cornish, V.W. (2002). Chemical complementation: a reaction-independent genetic assay for enzyme catalysis. Proc. Natl. Acad. Sci. USA *99*, 16537–16542.

Banaszynski, L.A., Liu, C.W., and Wandless, T.J. (2005). Characterization of the FKBP.rapamycin.FRB ternary complex. J. Am. Chem. Soc. *127*, 4715–4721.

Böhm, H.J., Banner, D., Bendels, S., Kansy, M., Kuhn, B., Müller, K., Obst-Sander, U., and Stahl, M. (2004). Fluorine in medicinal chemistry. ChemBioChem *5*, 637–643.

Bronson, J.E., Mazur, W.W., and Cornish, V.W. (2008). Transcription factor logic using chemical complementation. Mol. Biosyst. *4*, 56–58.

Cantley, L.C. (2002). The phosphoinositide 3-kinase pathway. Science *296*, 1655–1657.

Corson, T.W., Aberle, N., and Crews, C.M. (2008). Design and applications of bifunctional small molecules: why two heads are better than one. ACS Chem. Biol. *3*, 677–692.

Crabtree, G.R., and Schreiber, S.L. (1996). Three-part inventions: intracellular signaling and induced proximity. Trends Biochem. Sci. *21*, 418–422.

Deswal, S., Schulze, A.K., Höfer, T., and Schamel, W.W. (2011). Quantitative analysis of protein phosphorylations and interactions by multi-colour IP-FCM as an input for kinetic modelling of signalling networks. PLoS ONE *6*, e22928.

Edwards, S.R., and Wandless, T.J. (2007). The rapamycin-binding domain of the protein kinase mammalian target of rapamycin is a destabilizing domain. J. Biol. Chem. *282*, 13395–13401.

Faller, B. (2008). Artificial membrane assays to assess permeability. Curr. Drug Metab. *9*, 886–892.

Farrar, M.A., Alberol-Ila, J., and Perlmutter, R.M. (1996). Activation of the Raf-1 kinase cascade by coumermycin-induced dimerization. Nature *383*, 178–181.

Fili, N., Calleja, V., Woscholski, R., Parker, P.J., and Larijani, B. (2006). Compartmental signal modulation: Endosomal phosphatidylinositol 3-phosphate controls endosome morphology and selective cargo sorting. Proc. Natl. Acad. Sci. USA *103*, 15473–15478.

Gautier, A., Juillerat, A., Heinis, C., Corrêa, I.R.J., Jr., Kindermann, M., Beaufils, F., and Johnsson, K. (2008). An engineered protein tag for multiprotein labeling in living cells. Chem. Biol. *15*, 128–136.

Gautier, A., Nakata, E., Lukinavicius, G., Tan, K.T., and Johnsson, K. (2009). Selective cross-linking of interacting proteins using self-labeling tags. J. Am. Chem. Soc. *131*, 17954–17962.

Gendreizig, S., Kindermann, M., and Johnsson, K. (2003). Induced protein dimerization in vivo through covalent labeling. J. Am. Chem. Soc. *125*, 14970–14971.

Hinner, M.J., and Johnsson, K. (2010). How to obtain labeled proteins and what to do with them. Curr. Opin. Biotechnol. *21*, 766–776.

Idevall-Hagren, O., Dickson, E.J., Hille, B., Toomre, D.K., and De Camilli, P. (2012). Optogenetic control of phosphoinositide metabolism. Proc. Natl. Acad. Sci. USA *109*, E2316–E2323.

Inoue, T., and Meyer, T. (2008). Synthetic activation of endogenous PI3K and Rac identifies an AND-gate switch for cell polarization and migration. PLoS ONE *3*, e3068.

Inoue, T., Heo, W.D., Grimley, J.S., Wandless, T.J., and Meyer, T. (2005). An inducible translocation strategy to rapidly activate and inhibit small GTPase signaling pathways. Nat. Methods *2*, 415–418.

Kennedy, M.J., Hughes, R.M., Peteya, L.A., Schwartz, J.W., Ehlers, M.D., and Tucker, C.L. (2010). Rapid blue-light-mediated induction of protein interactions in living cells. Nat. Methods *7*, 973–975.

Keppler, A., Gendreizig, S., Gronemeyer, T., Pick, H., Vogel, H., and Johnsson, K. (2003). A general method for the covalent labeling of fusion proteins with small molecules in vivo. Nat. Biotechnol. *21*, 86–89.

Komatsu, T., Kukelyansky, I., McCaffery, J.M., Ueno, T., Varela, L.C., and Inoue, T. (2010). Organelle-specific, rapid induction of molecular activities and membrane tethering. Nat. Methods *7*, 206–208.

Lemercier, G., Gendreizig, S., Kindermann, M., and Johnsson, K. (2007). Inducing and sensing protein—protein interactions in living cells by selective cross-linking. Angew. Chem. Int. Ed. Engl. *46*, 4281–4284.

Levskaya, A., Weiner, O.D., Lim, W.A., and Voigt, C.A. (2009). Spatiotemporal control of cell signalling using a light-switchable protein interaction. Nature *461*, 997–1001.

Liang, F.S., Ho, W.Q., and Crabtree, G.R. (2011). Engineering the ABA plant stress pathway for regulation of induced proximity. Sci. Signal. *4*, rs2.

Liberles, S.D., Diver, S.T., Austin, D.J., and Schreiber, S.L. (1997). Inducible gene expression and protein translocation using nontoxic ligands identified by a mammalian three-hybrid screen. Proc. Natl. Acad. Sci. USA *94*, 7825–7830.

Lin, H., Abida, W.M., Sauer, R.T., and Cornish, V.W. (2000). Dexamethasone-Methotrexate: An Efficient Chemical Inducer of Protein Dimerization. J. Am. Chem. Soc. *122*, 4247–4248.

Liu, R., Liu, C.B., Mohi, M.G., Arai, K., and Watanabe, S. (2000). Analysis of mechanisms involved in the prevention of gamma irradiation-induced apoptosis by hGM-CSF. Oncogene *19*, 571–579.

Los, G.V., Encell, L.P., McDougall, M.G., Hartzell, D.D., Karassina, N., Zimprich, C., Wood, M.G., Learish, R., Ohana, R.F., Urh, M., et al. (2008). HaloTag: a novel protein labeling technology for cell imaging and protein analysis. ACS Chem. Biol. *3*, 373–382.

Merzlyak, E.M., Goedhart, J., Shcherbo, D., Bulina, M.E., Shcheglov, A.S., Fradkov, A.F., Gaintzeva, A., Lukyanov, K.A., Lukyanov, S., Gadella, T.W., and Chudakov, D.M. (2007). Bright monomeric red fluorescent protein with an extended fluorescence lifetime. Nat. Methods *4*, 555–557.

Miyamoto, T., DeRose, R., Suarez, A., Ueno, T., Chen, M., Sun, T.P., Wolfgang, M.J., Mukherjee, C., Meyers, D.J., and Inoue, T. (2012). Rapid and orthogonal logic gating with a gibberellin-induced dimerization system. Nat. Chem. Biol. *8*, 465–470.

Mohi, M.G., Arai, Ki., and Watanabe, S. (1998). Activation and functional analysis of Janus kinase 2 in BA/F3 cells using the coumermycin/gyrase B system. Mol. Biol. Cell *9*, 3299–3308.

O'Farrell, A.M., Liu, Y., Moore, K.W., and Mui, A.L. (1998). IL-10 inhibits macrophage activation and proliferation by distinct signaling mechanisms: evidence for Stat3-dependent and -independent pathways. EMBO J. *17*, 1006–1018.

O'Reilly, K.E., Rojo, F., She, Q.B., Solit, D., Mills, G.B., Smith, D., Lane, H., Hofmann, F., Hicklin, D.J., Ludwig, D.L., et al. (2006). mTOR inhibition induces upstream receptor tyrosine kinase signaling and activates Akt. Cancer Res. *66*, 1500–1508.

Rutkowska, A., Haering, C.H., and Schultz, C. (2011). A FlAsH-based cross-linker to study protein interactions in living cells. Angew. Chem. Int. Ed. Engl. *50*, 12655–12658.

Strickland, D., Lin, Y., Wagner, E., Hope, C.M., Zayner, J., Antoniou, C., Sosnick, T.R., Weiss, E.L., and Glotzer, M. (2012). TULIPs: tunable, light-controlled interacting protein tags for cell biology. Nat. Methods *9*, 379–384.

Varnai, P., Thyagarajan, B., Rohacs, T., and Balla, T. (2006). Rapidly inducible changes in phosphatidylinositol 4,5-bisphosphate levels influence multiple regulatory functions of the lipid in intact living cells. J. Cell Biol. *175*, 377–382.

Wullschleger, S., Loewith, R., and Hall, M.N. (2006). TOR signaling in growth and metabolism. Cell *124*, 471–484.

Wymann, M.P. (2012). PI3Ks-Drug Targets in Inflammation and Cancer. Subcell. Biochem. *58*, 111–181.

Wymann, M.P., and Marone, R. (2005). Phosphoinositide 3-kinase in disease: timing, location, and scaffolding. Curr. Opin. Cell Biol. *17*, 141–149.

Wymann, M.P., and Schneiter, R. (2008). Lipid signalling in disease. Nat. Rev. Mol. Cell Biol. *9*, 162–176.

Wymann, M.P., Zvelebil, M., and Laffargue, M. (2003). Phosphoinositide 3-kinase signalling—which way to target? Trends Pharmacol. Sci. *24*, 366–376.

Yazawa, M., Sadaghiani, A.M., Hsueh, B., and Dolmetsch, R.E. (2009). Induction of protein-protein interactions in live cells using light. Nat. Biotechnol. *27*, 941–945.

Zoncu, R., Efeyan, A., and Sabatini, D.M. (2011). mTOR: from growth signal integration to cancer, diabetes and ageing. Nat. Rev. Mol. Cell Biol. *12*, 21–35.